Case Studies in Construction Materials 16 (2022) e01062

Contents lists available at ScienceDirect

Case Studies in Construction Materials

journal homepage: www.elsevier.com/locate/cscm

Investigation of the effect of silica fume and synthetic foam additive on cell structure in ultra-low density foam concrete

Burçin Şenol Şeker [a], Murat Gökçe [a], Kenan Toklu [b,*]

[a] Faculty of Architecture, Amasya University, Amasya 05100, Turkey
[b] Çorlu Faculty of Engineering, Tekirdağ Namık Kemal University, Çorlu, Tekirdağ, Turkey

ARTICLE INFO

Keywords:
Foam concrete
Thermal conductivity coefficient
Silica fume
Ultra-low density
Synthetic foam additive
Cell structure

ABSTRACT

In this study, the properties of ultra-low density foam concrete with silica fume substitute and synthetic foam additive were investigated. Two different references and silica fume substituted foam concretes with densities of 220 and 200 kg/m^3 were produced. Silica fume was used as the replacement material and its ratio in the mixtures was kept constant at 5% by weight. According to the results of the study, the compressive strengths and the thermal conductivity coefficients of the references and silica fume substituted foam concretes with densities of 220 and 200 kg/m^3 were found to be 0.26, 0.21 and 0.32, 0.26 Mpa at 28 days and 0.073, 0.069 and 0.068, 0.060 W/mK, respectively. In addition, the behavior of foam concrete at high temperatures was investigated using a flame source, which can reach up to 1200 °C, since temperatures usually exceed 1000 °C during a fire. At the end of ten minutes, the heat permeability of silica fume substituted foam concrete exposed to a 1200 °C temperature was 6.5% and 5.3%, which was better than reference foam concretes, respectively. As a result, silica fume has positively affected the compressive strength at later ages and thermal conductivity properties of foam concrete.

1. Introduction

Foam concrete (FC), which has a porous structure, is a type of lightweight concrete obtained by mixing foam into cement mortar [1]. FC has been used at many construction sites since 1923 [1-6] in part because it is economical, but it is also environmentally friendly and fire resistant with low elasticity and acceptable thermal insulation [7-13].

The air void structure in FC is the most important factor on the compressive strength and dynamic modules of elasticity [14] As a natural result of the changes in the air void system, there may be significant effects on the micro/macro structure and mechanical properties of FC [15]. The literature [16] have shown that with the decrease in the density of FC, decreases in compressive strength occur. In addition, protein-based and two different synthetic-based foaming agents were used to produce FC. Therefore, the type of foaming agent used in FC production also affects the mechanical properties of FC [17].

In recent years, with the increase of studies for thermal-insulation materials used in buildings, the technological developments in this area have gradually accelerated. According to the principle of heat transfer [18-21], micro-porosity of the material to be used in thermal insulation is necessary in order to obtain good thermal insulation [18,22]. FC has excellent thermal insulation properties [23]. In the literature [16,24], when the cement-sand mortar and FC are compared, it has been reported that the thermal properties of FC with a density of 1000 kg/m^3 are six times more effective than the cement-sand mortar.

* Corresponding author.
E-mail addresses: senol.seker@amasya.edu.tr (B.Ş. Şeker), murat.gokce@amasya.edu.tr (M. Gökçe), ktoklu@nku.edu.tr (K. Toklu).

https://doi.org/10.1016/j.cscm.2022.e01062
Received 2 January 2022; Received in revised form 24 February 2022; Accepted 7 April 2022
Available online 8 April 2022
2214-5095/

Researchers have now begun increasing their work on the production of environmentally friendly and sustainable thermal insulation materials using waste products [25]. Silica fume (SF) is an inorganic byproduct used as a replacing material in concrete production and obtained from the metallurgical industry [26,27]. In the literature [28], it has been stated that SF improves early age strength of lightweight concretes but reduces workability.

This study sought to examine ultra-low-density FCs produced by replacing 5% of cement with SF, and investigate its effects on consistency, density, thermal conductivity coefficient and heat permeability properties.

2. Materials and methods

2.1. Materials

2.1.1. Cement and silica fume

The type of cement used in this study was CEM I 52.5 R with a density of 3.1 g/cm^3. The density of SF is 2.32 g/cm^3 and the surface area is 15,000 cm^2/g. Silica fume has been used to have a highly specific surface area and to fill the micro-voids by wrapping around the gaps more efficiently. Another reason for using SF is that it is a waste material, and will, therefore, not be as damaging to the environment. The properties of the cement and SF are presented in Table 1.

2.1.2. Chemical additive

Synthetic based foam additive was used in the study. The properties of this material are given in Table 2.

2.2. Method

FCs were first prepared as slurry (cement, water and ± SF). The cement, water and ± SF was stirred together in a helical type mixer with a speed of 40 rpm for 90 s (Fig. 1). The helical type mixer minimizes the damping of the foam and the volume losses that may occur in FC by reducing the mechanical effect that occurs. The solution prepared at the rate of 1/50 (1 unit of foam additive/50 units of water) in the foam generator was put into the foam tank reservoir (Fig. 2). Foam was then produced by having 2.5 bar compressed air blown into the foam solution inside the generator. Properties of the foam produced are given in Table 3. The prepared foam was placed in containers of certain volume and added to the slurry at the calculated rate and mixed in a helical type mixer for 90 s.

The quantity of materials used in FC production are given in Table 4. In addition, the foam volume amounts to be added to the foam concrete mixtures were calculated using Eqs. (1) and (2). The amount of foam volume to be added has been increased in order to reduce the unit volume weights in FCs. Then, a consistency test with a Marsh Funnel was performed on the freshly prepared FCs. After the foam concrete samples placed in the molds were removed the next day, they were left to cure. The curing period lasted 28 days. Afterward, compressive strength, microscope and SEM analysis, thermal conductivity and heat permeability tests under high temperature were performed on the hardened FCs.

2.2.1. Dry density measurement

Samples with size of 100×100×100 mm were weighted on 28th day. Then, the volumes of the samples were calculated. Lastly, dry densities of samples were calculated with Eq. (3) below.

$$\rho s = Ms/Vs \quad (3)$$

where,
ρs= Dry density (g/cm^3),
Ms= Weight of the samples after drying (g),
Vs= Volume of samples (cm^3).

2.2.2. Marsh cone flow test

The Marsh Cone Flow Test is used as the method to determine the flowability of fresh FC [29-31]. To conduct the test, the marsh

Table 1
Properties of CEM I 52.5 R and SF.

Oxide	Cement (w.-%)	SF (w.-%)
SO_3	3.27	1.3
SiO_2	21.7	82.7
Al_2O_3	4.06	4.34
Fe_2O_3	0.27	1.3
CaO	65.8	0.8
MgO	1.35	1.45
Na_2O	–	–
K_2O	–	–
LOI[a]	3.22	4.25

[a] LOI: Loss on ignition.

Table 2
Properties of synthetic based foam additive.

Density (g/cm^3)	Appearance	pH
1.20	Light brown	6

Fig. 1. Helical type mixer used in mixing foam concrete.

Fig. 2. Foam generator.

Table 3
Properties of foam.

Density (g/dm^3)	pH
85	6

Table 4
Mixture quantities.

Samples	Density kg/m^3	Bindercontent kg/m^3		Water content kg/m^3	Foam solution mixture ratio (Foam additive/water)	Volume of foam (%)
		C	SF			
C 200	200	170	–	85	1/50	85.8
C 220	220	180	–	95	1/50	85
CSF 200	200	161.5	8.5	85	1/50	85.8
CSF 220	220	172	8	95	1/50	85

Abbreviations
C: Cement
SF: Silica fume
C 220: Reference produced at density 220 kg/m^3
C 200: Reference produced at density 200 kg/m^3
CSF 220: Foam concrete produced at density of 220 kg/m^3 and has 5% silica fume
CSF 200: Foam concrete produced at density of 200 kg/m^3 and has 5% silica fume

$$\text{Foam Volume} = 1000\ \text{dm}^3 - \text{solid volume (dm}^3) \quad (1)$$

$$\text{Solid volume} = \text{Cement} \pm \text{silica fume} + \text{water volume} \quad (2)$$

cone is first filled with 1.5 liters of FC. The time it takes for 1 liter of FC to flow through the 10 mm hole is then measured [31,32] (Fig. 3). According to Table 5, if 1 liter of fresh FC is able to flow in less than one minute, the FC is considered to have a constant and regular flow. If the time exceeds one minute, it is expressed as interrupted or difficult flow; and if it does not flow at all, it is expressed as "no flow" [29,31-33].

2.2.3. Compressive strength test

A compressive strength test was applied to 100 × 100 × 100 mm cubic specimens on Days 1, 7, and 28 in accordance with TS EN 12390–3 [34] using a compressive strength test device at a speed of 2.0 ± 0.5 kN/s until the specimens were broken (Fig. 4).

2.2.4. Measurement of thermal conductivity

The thermal conductivity measurement for samples was carried out with a Thermtest HFM-100 test device (Fig. 5). Table 6 shows the properties of the device.

2.2.5. Flammability and heat permeability test

A temperature of approximately 1200 °C was applied to one surface of the FC slabs with dimensions of 300×300×50mm and the temperature change on the back surface was measured over the course of ten minutes with a laser heat meter [35]. A flame gun that can create a temperature of roughly 1300 °C, was used as the heat source (Fig. 6). A two-point laser heat meter that can measure the temperature change between 50 and 2200 °C remotely was used [35] (Fig. 7).

Fig. 3. Determination of consistency of foam concrete with The Marsh Cone Flow Test.

Table 5
Classification of foamed concrete flow [29,31-33].

Main Class	Description	Sub-class	Describtion
1	1 L < 1 min	A	Constant Flow
2	1 min < efflux < 2 min	B	Interrupted Flow
3	0.5 L<efflux< 1 L	C	
4	Efflux< 0.5 L		
5	No Flow		

Fig. 4. Test equipment for compressive strength test.

Fig. 5. Test tool used to determine the thermal conductivity coefficient.

Table 6
The properties of the device.

Specifications	Values
Plate Temperature Range	-20–70 °C
Maximum Sample Size	Up to 300 × 300×100 mm
High Thermal Conductivity Kit	Up to 2.5 W/m•K
Accuracy	Typically better than 3%
Thermal Conductivity Measuring Range	0.005–0.5 W/m•K
Measurement Time	30–60 min

Fig. 6. Flame gun used as a heat source.

Fig. 7. Laser remote temperature meter.

In the experiment, two heat sources (flame guns) were placed at equal distances away from the FC slabs (Fig. 6). After the flame guns were turned on, temperature changes were measured with a laser thermometer at intervals of one minute from the front surface where the heat source touched and the rear surface of the plate in the same direction (Fig. 7). The temperature change on the back surface was measured and recorded for ten minutes. At the end of the experiment, the ignition and burning conditions in FCs were observed and recorded.

3. Result and discussion

The fresh consistency of the FCs was determined with The Marsh Funnel. The obtained consistency results were classified according to Table 5. In this study, the consistency class for all samples was no flow. In ultra-low density FC, the air bubbles are closer to each other and the amount of solid material around the air bubbles is less. Since the surface loads of the air bubbles increase the mutual attraction power, the viscosity increased and the flow became difficult.

All FCs reached the strength to be released from the mold the next day and no volume loss or collapse occurred while waiting in the mold. One of the biggest threats to the preparation of low-density FCs is of its collapse while waiting in the mold. The foam added to the

Table 7
Test analysis of hardened foam concrete.

Samples	Fresh density (kg/m^3)	Hardened density (kg/m^3)	Thermal conductivity coefficient (W/mK)	Compressive Strength (MPa)		
				1 day	7 days	28 days
C 200	265	202	0.069	0.09	0.15	0.21
C 220	290	222	0.073	0.11	0.18	0.26
CSF 200	275	204	0.060	0.10	0.20	0.26
CSF 220	294	223	0.068	0.14	0.25	0.32

slurry must maintain its stability until the cement starts to harden. Otherwise, collapses occur in the molded foam concretes as a result of the damping of the foams that cannot maintain their stability, and this leads to volume losses. In this study, it was ensured that volume losses were prevented by using synthetic based foam additive and a helical type mixer.

According to Table 7, as the densities of the reference and SF substituted FCs decreased, their strengths also decreased. However, the compressive strength of CSF 200 was equal to the strength of C 220 in 28 days. This is due to the fact that the specific surface area of SF is higher than that of cement and its ability to surround voids more densely [36]. So, the void structures within the FC were improved by replacing cement with SF (Figs. 8 and 9). In this respect, the compressive strength of FC has increased with replacing cement with SF in later ages due to the pozzolanic effect of SF and the improvement of the void structures in the FC [16,37,38].

By examining Fig. 8 (the images of CSF 220 at 10- and 20-times magnification), it is clear that the resulting void diameters are much smaller and independent closed cells were formed. As a result of the highly specific surface area of the SF, its ability to surround small diameter air cells has increased. When Fig. 9 (the images of C 220 at 10- and 20-times magnification) is examined, it is should be noted that independent closed cells were formed, but there were no small-diameter void cells as in FCs with SF replacement.

Fig. 10 shows the SEM image of C 220 at 100 times magnification. Most of the voids formed in the FC were surrounded by cement and independent closed cells were formed. As a result of the independent closed cell formation and the increase in the capability of covering the voids by the cement, no collapse and volume losses occurred. It was determined that closed cells of different diameters between 178 and 976 μm were formed.

Fig. 11 shows the SEM image of CSF 220 at 100 times magnification. As seen from the SEM image, the majority of the voids formed were surrounded by cement and silica fume and independent closed cells were formed as they had been in C220. It is also evident in the SEM image that the highly specific surface area of the SF allows the creation of smaller diameter voids. It was determined that closed cells with different diameters between 64 and 515 μm were formed.

According to Table 7, the thermal conductivity coefficients for C 200, C 220, CSF 200 and CSF 220 were found 0.069, 0.073, 0.060 and 0.068 W/mK, respectively. The test result showed that the thermal conductivity reduces as the density decreases. Thus, it can be said that there is a relationship between density and thermal conductivity [39]. As seen in the SEM analysis of SF substituted FCs and Table 7, as a result of the formation of smaller diameter independent closed cells, SF substitution reduced the thermal conductivity. As the SF surrounds closed cells more intensely, the permeability of the barriers formed decreased. This result is similar to the work done by Demirboğa and Gül [40].

The effects of thermal permeability and burning conditions on FCs under high temperatures were tested in the heat permeability test [35]. Temperature values of experiment results are given in Table 8. When Table 8 and Fig. 12 are examined together, it is clear that no ignition or burning event occurred upon the FCs. The test method applied in this study will be useful in terms of getting quick results regarding the burning, ignition and heat permeability of lightweight thermal insulation materials. Also, by using this test method, information about the behavior of thermal insulation materials at high temperatures can be obtained quickly.

4. Conclusions

All FCs prepared did not show flowing in the marsh funnel test. In addition, there was no collapse or loss of volume in any of the FCs taken into the mold. As the unit volume weights decrease in FCs, the compressive strength has decreased. However, there has been an increase in the compressive strength of FCs with SF substitution. Thermal conductivity coefficient showed a direct relationship with the density of FC. As the density of the FCs decreased, the thermal conductivity coefficients reduced.

The thermal conductivity coefficient of CSF 200 was found to be 0.060 W/mK. According to this result, the FC in which SF is substituted can be included in the insulation material class. The high specific surface area of SF positively affected the compressive strength and thermal permeability properties of the FC as a result of the formation of independent closed cells by surrounding the walls of the voids in the FC more densely.

At the end of 10 min, the heat permeability of SF substituted FCs with densities of 220 and 200 kg/m^3 exposed to temperature at 1200 °C were respectively 6.5% and 5.3% better than reference foam concretes with densities of 220 and 200 kg/m^3. All FCs were

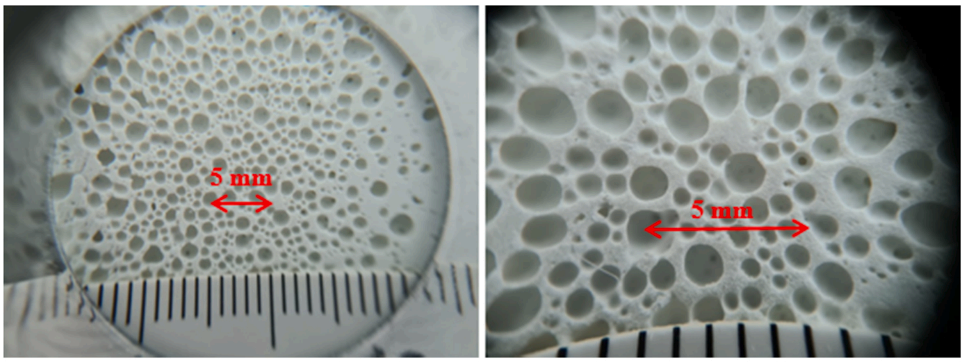

10x magnification 20x magnification

Fig. 8. Microscopic images of CSF 220.

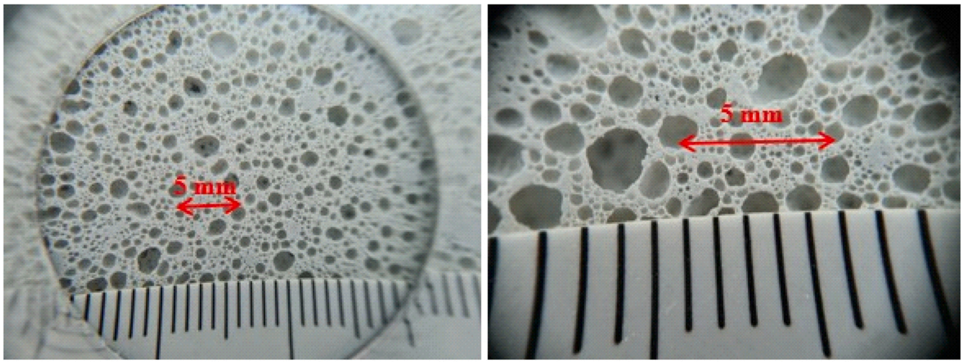

10x magnification 20x magnification

Fig. 9. Microscopic images of C 220.

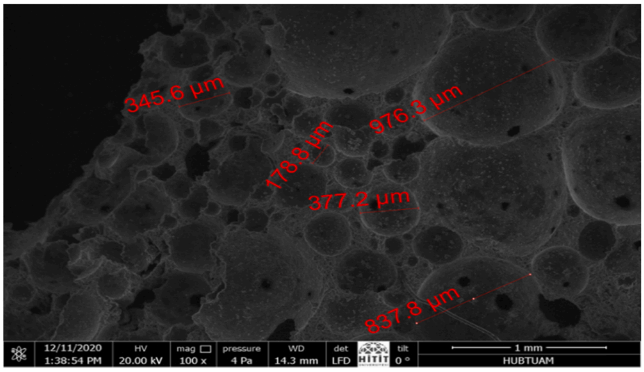

Fig. 10. SEM image of C 220 foam concrete.

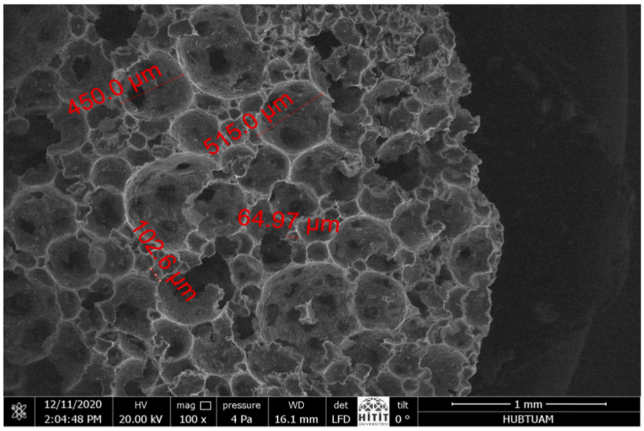

Fig. 11. SEM image of CSF 220 foam concrete.

exposed to 1200 °C temperature for 10 min and at the end of the test, they showed non-flammability. Since there is no flammable material in FC, it will not show any negative effect during fire.

In SEM analysis, smaller diameter (64 μm) cells were detected in more dense SF-substituted FCs. As a result of the surface area of SF being approximately 3 times more than cement, more smaller diameter cells were formed and these cells were surrounded more densely. As a result, the compressive strength, thermal conductivity coefficient and heat permeability test results of SF substituted FCs were better.

In short, FC can be used as a thermal insulation material with its workability, ease of application, low thermal conductivity coefficient and non-combustibility under high temperature effect.

Table 8
Temperature changes on the back surface of 300×300×50 mm foam concrete slabs.

Samples	Temperature Changes (°C)									
	1.min	2.min	3.min	4.min	5.min	6.min	7.min	8.min	9.min	10.min
C 200	21.6	22.3	23.2	24.3	25.8	27.3	29.2	29.9	30.5	31.9
C 220	21.8	23.8	24.6	25	29.6	31	31.6	32.4	33	33.9
CSF 200	21.1	22.7	22.9	23.5	23.9	25.6	26.8	27.9	29.1	30.2
CSF 220	21	22.9	23.5	24.4	25.1	27.8	28.3	29.2	30.4	31.7

(a) (b)

Fig. 12. (a) Back surface temperature measurement of foam concretes exposed to a temperature of about 1200 °C (b) The appearance of the samples after the experiment.

Declaration of Competing Interest

The authors declare that they have no known competing financial interests or personal relationships that could have appeared to influence the work reported in this paper.

References

[1] J. Gong, W. Zhang, The effects of pozzolanic powder on foam concrete pore structure and frost resistance, Constr. Build. Mater. 208 (2019) 135–143.
[2] S. Mindess. Developments in the Formulation and Reinforcement of Concrete, Second edition, Whoodhead Publishing, 2019, pp. 346–366.
[3] M.B. Youssef, F. Lavergne, K. Sab, K. Miled, J. Neji, Upscaling the elastic stiffness of foam concrete as a three-phase composite material, Cem. Concr. Res. 110 (2018) 13–23.
[4] M. Cong, C. Bing, Properties of a foamed concrete with soil as filler, Constr. Build. Mater. 76 (2015) 61–69.
[5] Y.H.M. Amran, N. Farzadnia, A.A.A. Ali, Properties and applications of foamed concrete; a review, Constr. Build. Mater. 101 (Part 1) (2015) 990–1005.
[6] M. Gökçe, B.Ş. Şeker, Foam concrete, J. N. Results Sci 9 (2020) 9–18.
[7] F. Oginni, Continental application of foamed concrete technology: lessons for infrastructural development in Africa, Br. J. Appl. Sci. Technol. 5 (4) (2015) 417–424.
[8] J. Gong, L. Zhu, J. Li, D. Shi, Silica fume and nanosilica effects on mechanical and shrinkage properties of foam concrete for structural application, Adv. Mater. Sci. Eng. 2020 (2020) 1–10.
[9] Z. Zhang, J.L. Provis, A. Reid, H. Wang, Geopolymer foam concrete: an emerging material for sustainable construction, Constr. Build. Mater. 56 (2014) 113–127.
[10] L. Chica, A. Alzate, Cellular concrete review: new trends for application in construction, Constr. Build. Mater. 200 (2019) 637–647.
[11] T. Li, F. Huang, J. Zhu, J. Liu, Effect of foaming gas and cement type on the thermal conductivity of foamed concrete, Constr. Build. Mater. 231 (2020), 117197.
[12] A. Raj, D. Sathyan, K.M. Mini, Physical and functional characteristics of foam concrete: a review, Constr. Build. Mater. 221 (2019) 787–799.
[13] I.X. Alex, K. Arunachalam, Flexural behavior of fiber reinforced lightweight concrete, Rev. De. la Constr. 18 (3) (2019) 536–544.
[14] H.K. Kim, J.H. Jeon, H.K. Lee, Workability, and mechanical, acoustic and thermal properties of lightweight aggregate concrete with a high volume of entrained air, Constr. Build. Mater. 29 (2012) 193–200.
[15] T.H. Wee, D.S. Babu, T. Tamilselvan, H.S. Lim, Air-void system of foamed concrete and its effect on mechanical properties, ACI Mater. J. 103 (1) (2006) 45–52.
[16] K. Ramamurthy, E.K. Nambiar, G.I.S. Ranjani, A classification of studies on properties of foam concrete, Cem. Concr. Compos. 31 (6) (2009) 388–396.
[17] D.K. Panesar, Cellular concrete properties and the effect of synthetic and protein foaming agents, Constr. Build. Mater. 44 (2013) 575–584.
[18] J. Han, G. Li, H. Gao, S. Chen, L. Tian, L. Yuan, Foaming mechanisms of different foaming agents and their effects on the microstructures of porous magnesia ceramics, J. Aust. Ceram. Soc. 56 (2020) 1005–1011.
[19] H. Schneider, J. Schreuer, B. Hildmann, Structure and properties of mullite – a review, J. Eur. Ceram. Soc. 28 (2) (2008) 329–344.
[20] W. Pabst, E. Gregorová, Conductivity of porous materials with spheroidal pores, J. Eur. Ceram. Soc. 34 (11) (2014) 2757–2766.
[21] W. Pabst, E. Gregorová, A cross-property relation between the tensile modulus and the thermal conductivity of porous materials, Ceram. Int. 33 (1) (2007) 9–12.
[22] N.D. Ngo, K.K. Tamma, Computational developments for simulation based design:multi-scale physics and flow/thermal/cure/stress modeling analysis, and validation for advanced manufacturing of composites with complex microstructures, Arch. Comput. Methods Eng. 10(1–2) (2003) 201–206.
[23] N. Silva, U. Mueller, K. Malaga, P. Hallingberg, C. Cederqvist, C. (2015). Foam concrete-aerogel composite for thermal insulation in lightweight sandwich facade elements. In 27th biennial national conference of the concrete institute of Australia in conjunction with the 69th RILEM Week.

[24] D. Aldridge, T. Ansell, (2001) Foamed concrete: production and equipment design, properties, applications and potential. In: Proceedings of one day seminar on foamed concrete: properties, applications and latest technological developments. Loughborough University, (pp.1-7).
[25] E. Papa, V. Medri, D. Kpogbemabou, V. Morinière, J. Laumonier, A. Vaccari, S. Rossignol, Porosity and insulating properties of silica-fume based foams, Energy Build 131 (2016) 223–232.
[26] ACI Committee116, Reported by ACI Committee 116, Cement and concrete terminology. American Concrete Institute, 2000.
[27] Y. Luna-Galiano, C. Leiva, C. Arenas, C. Fernández-Pereira, Fly ash based geopolymeric foams using silica fume as pore generation agent. Physical, mechanical and acoustic properties, J. Non-Cryst. Solids 500 (2018) 196–204.
[28] B. Chen, J. Liu, Experimental application of mineral admixtures in lightweight concrete with high strength and workability, Constr. Build. Mater. 22 (6) (2008) 1108–1113.
[29] İ. Demir, M.S. Başpinar, E. Kahraman, Experimental investigation of foam concrete rheological properties, Cumhur. Univ. Fac. Sci. Sci. J 38 (1) (2017) 109–118.
[30] N. Rousesel, Rheology of fresh concrete: from measurements to predictions of casting processes, Mater. Struct. 40 (10) (2007) 1001–1012.
[31] R.K. Dhir, M.R. Jones, L.A. Nicol, Development of structural grade foamed concrete. Final Report, DETR Research Contract 39/3/385,1999, pp. 84.
[32] M.R. Jones, M.J. McCarthy, A. McCarthy, Moving fly ash utilization in concrete forward: a UK perspective. In Proceedings of the 2003 International Ash Utilization Symposium, Centre for Applied Energy Research, University of Kentucky, 2003, pp. 20–22.
[33] M. Maziah, Development of foamed concrete: enabling and supporting design. A thesis presented in application for the degree of doctor of philosophy Division of Civil Engineering University of Dundee, 2011.
[34] TS EN 12390-3, Testing hardened concrete - Part 3: Compressive strength of test specimens. Turkish Standard, Ankara, 2019.
[35] M. Gökçe, K. Toklu, Ultra-low density foam concrete production using electrolyzed water, J. Test. Eval. 50 (2) (2022) 1212–1223.
[36] M. Panjehpour, A.A.A. Ali, R. Demirboga, A review for characterization of silica fume and its effects on concrete properties, Int. J. Sustain. Constr. Eng. Technol. 2 (2) (2011).
[37] Z.M. Yaseen, R.C. Deo, A. Hilal, A.M. Abd, L.C. Bueno, S. Salcedo-Sanz, M.L. Nehdi, Predicting compressive strength of lightweight foamed concrete using extreme learning machine model, Adv. Eng. Softw. 115 (2018) 112–125.
[38] A.A. Hilal, N.H. Thom, A.R. Dawson, On void structure and strength of foamed concrete made without/with additives, Constr. Build. Mater. 85 (2015) 157–164.
[39] O. Sengul, S. Azizi, F. Karaosmanoglu, M.A. Tasdemir, Effect of expanded perlite on the mechanical properties and thermal conductivity of lightweight concrete, Energy Build. 43 (2-3) (2011) 671–676.
[40] R. Demirboğa, R. Gül, The effects of expanded perlite aggregate, silica fume and fly ash on the thermal conductivity of lightweight concrete, Cem. Concr. Res. 33 (5) (2003) 723–727.